

Electronic structures of Hg-doped anatase TiO₂ with different O vacancy concentrations

S.K. ZHENG*, GUOHAO WU, SUOLIANG ZHANG, JIE SU, LEI LIU, FANG WANG, RUI ZHAO, XIAOBING YAN

Research Center for Computational Materials & Device Simulations, College of Electronic & Informational Engineering, Hebei University, Baoding 071002, P.R. China

The electronic structures of Hg-doped anatase TiO₂ with different O vacancy concentrations were calculated using the first-principles based on the density functional theory. The calculated results show that the forbidden band widths of Hg-doped anatase TiO₂ widened along with the increase of O vacancy concentration, which is responsible for the blue shift in the absorption edges. It can be deduced from the present study that the Hg-doped TiO₂ samples prepared in the experimental research contain a certain quantity of O vacancies.

Keywords: *Hg doping; anatase TiO₂; O vacancy; first-principles*

© Wrocław University of Technology.

1. Introduction

TiO₂ has been widely investigated for its potential applications in the fields of solar energy conversion, environmental cleaning, and planar waveguides [1–3]. In order to improve the performance of TiO₂, it is necessary to introduce active ions into the lattice of TiO₂. For example, P doping can slow down the growth of anatase particles and increase the anatase-to-rutile phase transformation temperature to more than 900 °C, which results in the higher photocatalytic activity for the degradation of 4-chlorophenol [4]; S doping can make a clear reduction in the band gap energy of S-doped TiO₂ photoanode compared to the band gap value for P25 and leads to a conversion efficiency of 6.91 % for the dye-sensitized solar cells which is 24 % higher than that of the undoped solar cells [5]; Al- and V-doping can increase the resistance of TiO₂ nanofilms upon to the exposure of hydrogen-containing atmosphere and show good sensitivity at both room temperature and evaluated temperatures [6].

To understand the property changes resulted from the active ions doping, many theoretical cal-

culations have been carried out using the first-principles based on density functional theory. Theoretical calculations indicate that the strong hybridization of Ti 3*d* states with W 5*d* states is the dominating factor to cause the shift in Fermi level into conduction band which results in the minimum resistivity of W-doped anatase TiO₂ [7]. First-principles calculations also confirm the formation of Ti 3*d* gap states when N concentration exceeds 1 at % in the N-doped TiO₂, which leads to the pinging of N 2*p* states in the band gap [8]. The origin of the visible-light activity of TiO₂ doped with carbonate species was studied using the plane-wave-based pseudopotential density functional theory calculations [9]. The results show that the carbonate species doped TiO₂ exhibits excellent absorption in the visible-light region of 400 nm to 800 nm, which is in good agreement with experimental observations.

Recently, Hg ions were successfully introduced into TiO₂ thin films and the samples showed different optical properties compared with the undoped ones [10, 11]. The structure and semiconducting properties of TiO₂ films were strongly modified by the Hg impurities. It was found that the optical band gap of Hg-doped anatase TiO₂ became narrower with the annealing temperature in-

*E-mail: zhshk@126.com

crease. This phenomenon, the authors ascribed to the change in the film density and the increase in grain size but did not give any theoretical analysis. Therefore, the electronic structures of Hg-doped anatase TiO_2 with different O vacancy concentration were calculated using the first-principles based on the density functional theory to explain the optical results obtained in the experimental research and the calculated results were discussed.

2. Computational details

The Hg-doped TiO_2 annealed at 400 °C to 800 °C is in anatase phase and the Hg doping concentration is kept as constant of $\text{Hg}:(\text{Hg} + \text{Ti}) = 5\%$ [10]. So, a 108 atoms $3 \times 3 \times 1$ anatase TiO_2 supercell was selected to perform the calculations, as shown in Fig. 1. For constructing Hg-doped anatase TiO_2 (Hg-TiO_2) with different O vacancy concentrations, the Ti atom marked as “A” was substituted by a Hg atom, then the O atoms marked as “O1”, “O2”, “O3”, and “O4” were deleted one by one to form Hg-TiO_2 with one O vacancy ($\text{Hg}/1\text{O}_v\text{-TiO}_2$) [12], two O vacancies ($\text{Hg}/2\text{O}_v\text{-TiO}_2$), three O vacancies ($\text{Hg}/3\text{O}_v\text{-TiO}_2$), and four O vacancies ($\text{Hg}/4\text{O}_v\text{-TiO}_2$), respectively.

First-principles calculations were carried out within the generalized gradient approximation using the Perdew-Burke-Ernzerhof exchange correlation potential. The code is implemented in the CASTEP [13]. The valence atomic configurations are $2s^22p^6$ for O, $3s^23p^63d^24s^2$ for Ti, and $5d^{10}6s^2$ for Hg. An energy cutoff of 300 eV and a Monkhorst-Pack k -mesh of $2 \times 2 \times 2$ is used. All of the structures were allowed to relax with a convergence threshold for the maximum energy change of 2.0×10^{-5} eV/atom, and the maximum force, maximum stress and displacement tolerances were set as 0.05 eV/Å, 0.1 GPa, and 0.002 Å, respectively.

After structural optimization, the electronic energy band structures, the partial density of states (PDOS), and the absorption spectra of the Hg-doped anatase TiO_2 with different O vacancy concentrations were calculated.

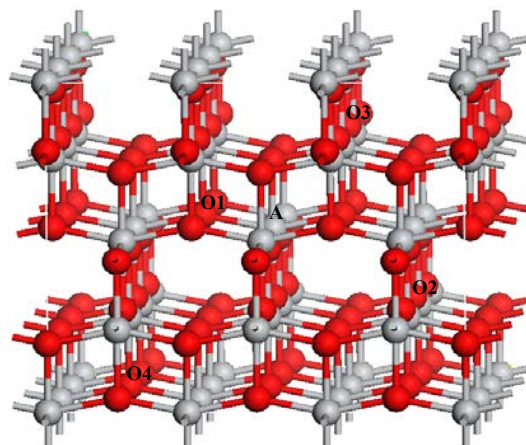


Fig. 1. Structural model of the anatase TiO_2 .

3. Results and discussion

In a previous work, we have shown the calculated results of Hg-TiO_2 and $\text{Hg}/1\text{O}_v\text{-TiO}_2$ [12]. For contrast, some results were cited herein.

Firstly, the volumes of the supercells and the net charges of Hg were calculated for the series of Hg-doped TiO_2 with different O vacancy concentration, as shown in Table 1.

From Table 1 it can be seen that the volume of the supercell becomes larger along with the increase in O vacancy concentration. That is to say, although the total number of atoms in the supercell decreases, the volume of the supercell increases. The reasons can be ascribed to the following: 1) the incorporation of Hg into anatase TiO_2 increases the strain [10], the strain releasing during the structural relaxation increases the volume of the supercell; 2) the increase of O vacancy concentration further adds more local strain to the supercell, the releasing of the additional strain increases the volume of the supercell.

The net charges of Hg decrease with the increase in the O vacancy concentration. This phenomenon is easy to understand. As there are less O atoms in the supercell when the O vacancy concentration increases, the Hg will lose less electrons because less O will attract less electrons. Therefore, the net charge of Hg becomes smaller when the O vacancy concentration increases.

Table 1. Volumes and Hg charges.

	Hg/1O _v -TiO ₂ [12]	Hg/2O _v -TiO ₂	Hg/3O _v -TiO ₂	Hg/4O _v -TiO ₂
Volume	1306.24 Å ³	1319.19 Å ³	1330.55 Å ³	1342.19 Å ³
Charge	1.55 e	1.02 e	1.00 e	0.95 e

3.1. Structures of energy band

The band structures near the Fermi energy level of the Hg/(1 - 4)O_v-TiO₂ are shown in Fig. 2. The energy zero point was set as the highest level filled up by the electrons.

From Fig. 2 it can be seen that the forbidden band width of the Hg-doped TiO₂ becomes larger with the increase in the O vacancy concentration. There is only one impurity energy level about 0.18 eV above the valence band maximum (VBM) in the Hg/1O_v-TiO₂. For the Hg/2O_v-TiO₂, the single doping energy level exists at the position of about 1.2 eV above the VBM. While for the Hg/3O_v-TiO₂ and Hg/4O_v-TiO₂, the highest energy level filled up by the electrons incorporates into the conduction band minimum (CBM), it means the semiconductor properties of the doping systems are changed. There is also a single doping energy level that appears between the VBM and CBM both in the Hg/3O_v-TiO₂ (about 1.17 eV above the VBM) and in the Hg/4O_v-TiO₂ (about 1.11 eV above the VBM).

The enlargement of the energy band gap will result in the blue shift of the optical absorption edges. Then, from the calculated results it can be deduced that the absorption edges of the Hg-doped anatase TiO₂ will show more and more blue shift with the increase of the O vacancy concentration, which will be identified by the absorption spectral calculations.

Mechiakh et al. [10] have reported that when Hg-doped TiO₂ was annealed from 400 °C to 800 °C, the structure was completely anatase phase. As the authors kept the Hg doping concentration at a constant value of 5 %, the optical band gaps for the Hg-doped anatase TiO₂ annealed at 800 °C, 600 °C, and 400 °C are 3.46 eV, 3.51 eV, and 3.57 eV, respectively. That is to say, lower annealing temperature will increase the op-

tical band gap of the Hg-doped TiO₂. From the fact that the calculated band gaps of the Hg/1O_v-TiO₂, Hg/2O_v-TiO₂, Hg/3O_v-TiO₂, and Hg/4O_v-TiO₂ are 2.32 eV, 2.39 eV, 2.47 eV, and 2.61 eV, respectively, it is obvious that the band gaps increase with the increase of O vacancy concentration. The experimental results and the calculated results have the same tendency. As we know, TiO₂ is an n-type semiconductor with intrinsic O defects. From the present calculated results and considering that the annealing process was carried out at ambient atmosphere [10], it can be deduced that the Hg-doped anatase TiO₂ thin films, prepared in the experiment, contain a certain number of O vacancies whose concentration will decrease with the annealing temperature rise.

3.2. Partial density of states

In order to analyze the components of the doping energy levels in the Hg-doped anatase TiO₂ with different O concentration, the electronic partial density of states (PDOS) near the energy zero point was calculated, as shown in Fig. 3.

From Fig. 3 it can be seen that the PDOS spectra are very different. The doping energy level in Hg/1O_v-TiO₂ is mainly caused by the contributions of Hg 5*d* and O 2*p* orbitals. For the Hg/2O_v-TiO₂, it is obvious that the impurity energy level comes from the hybridization of Hg 6*s* and O 2*p* orbital. For Hg/3O_v-TiO₂, the impurity energy level between the VBM and CBM is composed of hybridized Hg 6*s* and O 2*p* orbital, another doping energy level, lying in the conduction band, results from the contributions of Ti 3*d* electron. For the Hg/4O_v-TiO₂, its impurity energy levels are similar to the Hg/3O_v-TiO₂, but the relative positions of the impurity energy levels are different.

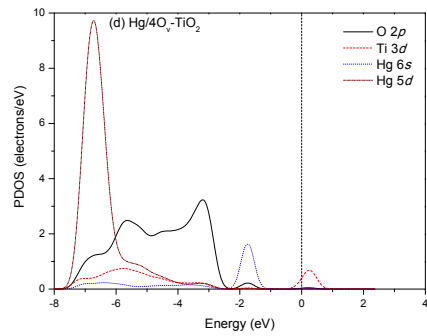
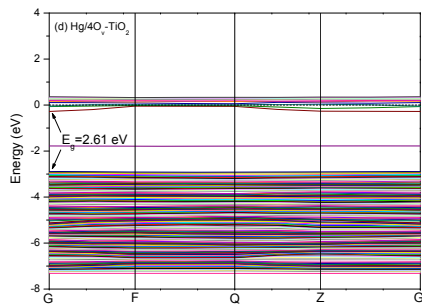
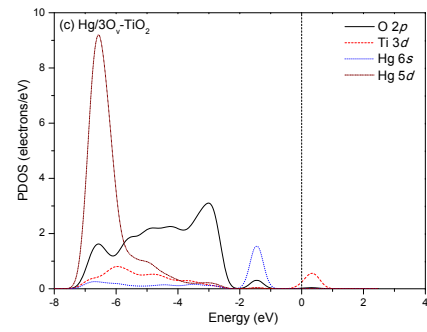
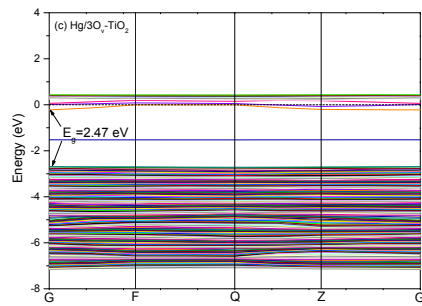
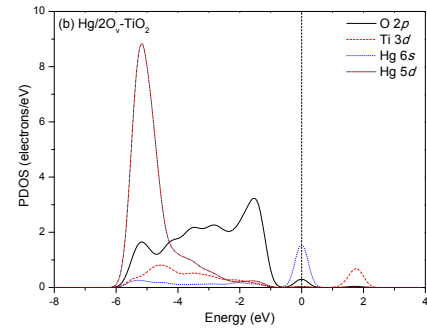
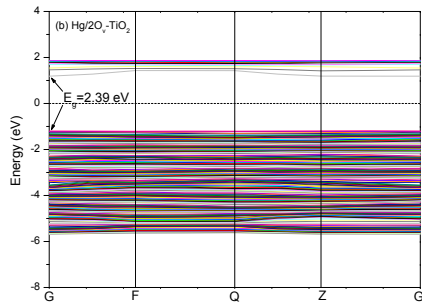
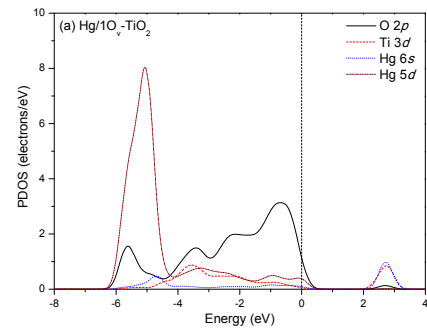
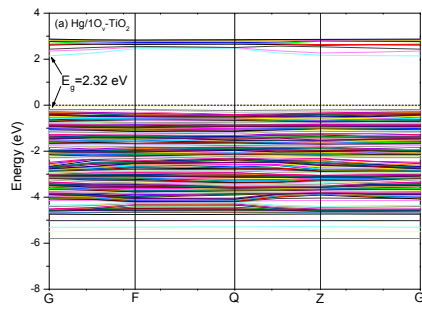


Fig. 2. Structures of energy band of the Hg/1O_v-TiO₂ [12] (a), Hg/2O_v-TiO₂ (b), Hg/3O_v-TiO₂ (c), Hg/4O_v-TiO₂ (d).

Fig. 3. PDOS of the Hg/1O_v-TiO₂ [12] (a), Hg/2O_v-TiO₂ (b), Hg/3O_v-TiO₂ (c), Hg/4O_v-TiO₂ (d).

3.3. Absorption spectra

The absorption spectra of the Hg/(1 - 4)O_v-TiO₂ are shown in Fig. 4. It is very clear that all of the doped systems show blue shift in the violet light region. The degree of blue shift becomes larger with the increase of the O vacancy concentration. This is in agreement with the calculated results of the band gaps. In the visible light region, both Hg/3O_v-TiO₂ and Hg/4O_v-TiO₂ show significant absorption ability, which is possibly due to the impurity energy level between the VBM and the CBM.

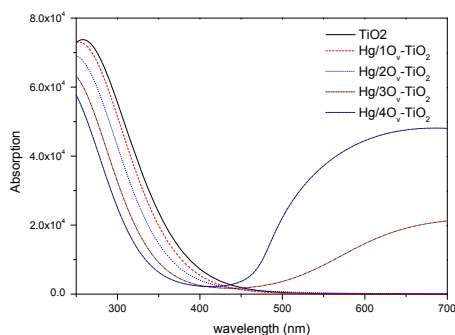


Fig. 4. Absorption spectra of the Hg-doped anatase TiO₂ with different O vacancies.

4. Conclusion

The energy band structures, electronic partial density of states, absorption spectra of Hg-doped anatase TiO₂ with different O vacancy concentrations were calculated using the first-principles based on the density functional theory. The results indicate that the band gaps become larger with the increase in the O vacancy concentration. For Hg/1O_v-TiO₂ and Hg/2O_v-TiO₂, only one impurity energy level appears between the VBM and CBM. While for Hg/3O_v-TiO₂ and Hg/4O_v-TiO₂, both of them have two impurity energy levels. The absorption spectra show larger blue shift with the

increase of O vacancy concentration. The results provide a proof for the existence of O vacancy in the Hg-doped TiO₂ samples prepared in the experimental research.

Acknowledgements

This work is financially supported by the National Natural Science Foundation of China (Grant No. 61306098), Hebei Province Natural Science Foundation (Grant No. E2012201088, F2013201196) and the Science Research Program of University in Hebei Province (Grant No. ZH2012019). We highly acknowledge our group leader Baoting Liu for his helpful discussions and CASTEP software assistance.

References

- [1] HOANG S., BURGLUND S.P., FULLON R.R., MINTER R.L., MULLINS B.C., *J. Mater. Chem. A*, 1 (2013), 4307.
- [2] LIANG F.X., KELLY T.L., LUO L.B., LI H., SAILOR M.J., LI Y.Y., *ACS Appl. Mater. Inter.*, 4 (2012), 4177.
- [3] KAWACHI M., *Electron. Lett.*, 19 (1983), 583.
- [4] ELGHNIJI K., HENTATI O., MLAIK N., MAHFOUDH A., KSIBI M., *J. Environ. Sci.*, 24 (2012), 479.
- [5] SUN Q., ZHANG J., WANG P.Q., ZHENG J., ZHANG X.N., CUI Y.Z., FENG J.W., ZHU Y.J., *JRSE*, 4 (2012), 023104-1.
- [6] LI Z.H., DING D.Y., NING C.Q., *Nanoscale Res. Lett.*, 8 (2013), 25.
- [7] CHEN D.M., XU G., MIAO L., CHEN L.H., NAKAO S., JIN P., *J. Appl. Phys.*, 107 (2010), 063707-1.
- [8] CHAI J.W., YANG M., CHEN Q., PAN J.S., ZHENG Z., FENG Y.P., WANG S.J., *J. Appl. Phys.*, 109 (2011), 023707-1.
- [9] TIAN F.H., LIU C.B., ZHANG D.Q., FU A.P., DUAN Y.B., YUAN S.P., YU J.C., *Chemphyschem*, 11 (2010), 3269.
- [10] MECHIAKH R., SEDRINE N.B., KARYOUI M., CHTOUROU R., *Appl. Surf. Sci.*, 257 (2011), 5529.
- [11] MECHIAKH R., SEDRINE N.B., CHTOUROU R., *Appl. Surf. Sci.*, 257 (2011), 9103.
- [12] ZHENG S.K., WU G.H., LIU L., *Solid State Commun.*, 165 (2013), 15.
- [13] CLARK S.J., SEGALL M.D., PICKARD C.J., HASNIP P.J., PROBERT M.J., REFSON K., PAYNE M.C., *Z. Kristallogr.*, 220 (2005), 567.

Received 2013-03-27

Accepted 2014-01-03